

Dynamics of F=2 Spinor Bose-Einstein Condensates

H. Schmaljohann, M. Erhard, J. Kronjäger, M. Kottke¹, S. van Staa, J. J. Arlt¹, K. Bongs, and K. Sengstock

Institut für Laser-Physik, Universität Hamburg, Luruper Chaussee 149, 22761 Hamburg, Germany

¹ *Institut für Quantenoptik, Universität Hannover, Welfengarten 1, 30167 Hannover, Germany*

(Dated: November 14, 2018)

We experimentally investigate and analyze the rich dynamics in F=2 spinor Bose-Einstein condensates of ⁸⁷Rb. An interplay between mean-field driven spin dynamics and hyperfine-changing losses in addition to interactions with the thermal component is observed. In particular we measure conversion rates in the range of $10^{-12} \text{ cm}^3 \text{ s}^{-1}$ for spin changing collisions within the F=2 manifold and spin-dependent loss rates in the range of $10^{-13} \text{ cm}^3 \text{ s}^{-1}$ for hyperfine-changing collisions. From our data we observe a polar behavior in the F=2 ground state of ⁸⁷Rb, while we measure the F=1 ground state to be ferromagnetic. Furthermore we see a magnetization for condensates prepared with non-zero total spin.

PACS numbers: 03.75.Mn, 34.50.Pi, 03.75.Hh

The investigation of atomic spin systems is central for the understanding of magnetism and a highly active area of research e.g. with respect to magnetic nanosystems, spintronics and magnetic interactions in high T_c superconductors. In addition entangled spin systems in atomic quantum gases show intriguing prospects for quantum optics and quantum computation [1, 2, 3, 4, 5]. Bose-Einstein condensates (BEC) of ultra-cold atoms offer new regimes for studies of collective spin phenomena [6, 7, 8, 9, 10, 11, 12, 13]. BECs with spin degree of freedom are special in the sense that their order parameter is a vector in contrast to the “common” BEC where it is a scalar. Recent extensive studies have been made in optically trapped ²³Na in the F=1 state [10, 11, 12, 13]. In addition evidence of spin dynamics was demonstrated in optically trapped ⁸⁷Rb in the F=1 state [14]. There is current interest in extending the systems under investigation to F=2 spinor condensates [15, 16, 17, 18, 19, 20], which add significant new physics. F=2 spinor condensates offer richer dynamics, an additional magnetic phase, the so-called cyclic phase [16, 18], as well as intrinsic connections to d-wave superconductors [21].

In this letter we present first studies of optically trapped ⁸⁷Rb F=2 spinor condensates. We measure rates for spin changing collisions for different channels within the F=2 manifold and discuss the steady state for various initial conditions. Additionally we observe and discuss the thermalization of dynamically populated m_F condensates. We also present measurements of spin-dependent hyperfine decay rates of the F=2 state in ⁸⁷Rb, as a key to further understanding the intensively studied collisional properties of ⁸⁷Rb [22, 23].

Our experimental setup consists of a compact double MOT apparatus which produces magnetically trapped ⁸⁷Rb Bose-Einstein condensates containing 10^6 atoms in the F=2, $m_F = 2$ state. To confine the atoms independently of their spin state they are subsequently transferred into a far detuned optical dipole trap. It is operated at 1064 nm generating trapping frequencies of typ-

ically $2\pi \times 891 \text{ Hz}$ vertically, $2\pi \times 155 \text{ Hz}$ horizontally and $2\pi \times 21.1 \text{ Hz}$ along the beam direction. After transfer we further cool the ensemble for 500 ms by selective parametric excitation [24] resulting in approximately 10^5 optically trapped atoms and a condensate fraction well above 60%. We are able to prepare arbitrary spin compositions using rapid adiabatic passage and controlled Landau-Zener crossing techniques [25] at an offset field around 25 G. After initial state preparation the magnetic field is lowered to a value of typically $340(\pm 20) \text{ mG}$, with a field gradient below 15 mG/cm , to ensure a well-defined quantization axis and a good overlap of the different m_F states during spin dynamics [26]. Spin dynamics is subsequently allowed to proceed during a variable hold time: Stored in the optical trap the condensate spin degree of freedom can evolve under well-controlled conditions. Due to interatomic interactions, initially prepared m_F components can evolve into other m_F components, e.g. by processes like $|0\rangle + |0\rangle \leftrightarrow |+1\rangle + |-1\rangle$, while - disregarding atomic losses - the total spin is conserved. This process is expected to end in the spinor ground state distribution showing the hyperfine dependent magnetic properties of the atomic species under investigation. Experimentally we detect different spin components by spatially separating them with a Stern-Gerlach method during time of flight (after switching off the trapping potential). Absorption imaging is then used to evaluate the respective spatial density distributions as well as the number of atoms in the condensate and thermal fractions for each spin component. Figure 1 shows typical spinor condensate evolutions for different starting conditions. These pictures demonstrate a rich spectrum of spin dynamics in F=2 systems, caused by an intriguing interplay of spin component coupling and spin-dependent losses. In the following we will investigate these processes separately.

We analyze the observed spinor evolution following a mean-field approach [16, 18, 27], in which the properties of a spinor condensate are determined by a spin-dependent energy functional. Extending the approach of

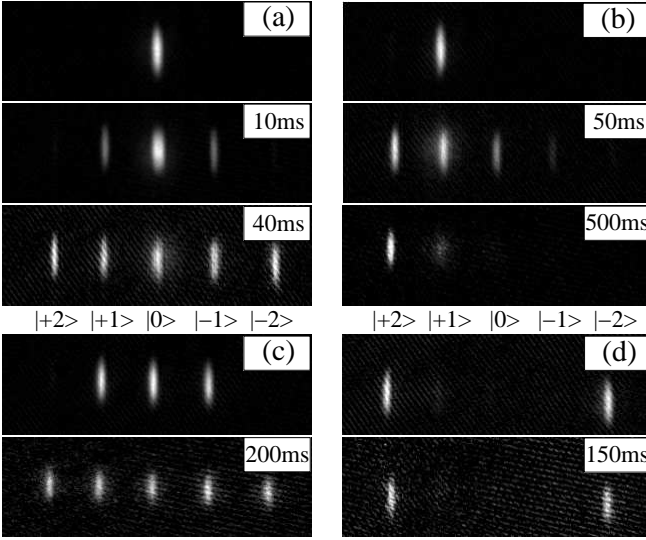


FIG. 1: Time-dependent observation of different m_F components starting from the initially prepared states denoted by (a)-(d). Shown are spinor condensates separated by a Stern-Gerlach method (time of flight 31ms).

[18] by the experimentally relevant quadratic Zeeman energy term we determine the following functional for $F=2$ systems:

$$K_{spin} = c_1 \langle \mathbf{F} \rangle^2 + \frac{4}{5} c_2 |\langle s_- \rangle|^2 - p \langle F_z \rangle - q \langle F_z^2 \rangle, \quad (1)$$

where $\langle \mathbf{F} \rangle$, $\langle F_z \rangle$ and $\langle s_- \rangle$ denote the expectation values for the spin vector, its z component and the spin-singlet pair amplitude. The experimentally controllable parameters p and q span the phase space for the system. Here p represents the mean spin of the system while q is the quadratic Zeeman energy, representing the magnetic offset field.

The spin-dependent mean-field is characterized by the parameters $c_1 = \frac{4\pi\hbar^2}{m} \cdot \frac{a_4 - a_2}{7}$ and $c_2 = \frac{4\pi\hbar^2}{m} \cdot \frac{7a_0 - 10a_2 + 3a_4}{7}$, introducing the s-wave scattering length a_f for collisions involving a total spin f of the colliding pair. In the following the $F = 2, m_F = X$ state is denoted by $|X\rangle$. For simplicity relative phases in mixtures are neglected. The c_1 term includes all couplings of states with $\Delta m_F = \pm 1$, e.g. $|0\rangle + |0\rangle \leftrightarrow |+1\rangle + |-1\rangle$. The c_2 term includes the only possible coupling with $\Delta m_F = \pm 2$: $|0\rangle + |0\rangle \leftrightarrow |+2\rangle + |-2\rangle$. The magnitude of these terms is connected to the timescales of spin dynamics and their relative strengths indicate the initially dominant channels. Taking the calculated scattering lengths and our initial experimental conditions (offset field $B = 340$ mG, mean density $n \approx 1.1 \times 10^{14} \text{ cm}^{-3}$) the energy ranges for the different terms are: spin independent mean-field $k_B \times 64$ nK, spin-dependent mean-field c_1 : $k_B \times 0.12$ nK, c_2 : $k_B \times 0.05$ nK and quadratic Zeeman energy q : $k_B \times 0.16$ nK.

Minimizing the energy functional, Eq. (1) leads to the

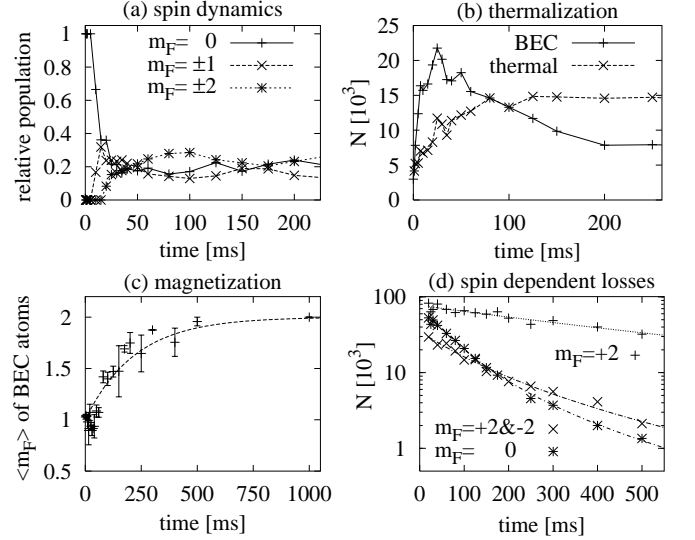


FIG. 2: Spin dynamics and spin-dependent losses. (a) Relative population of the m_F states of a condensate initially prepared in $|0\rangle$. (b) Thermalization of a BEC in the $|+2\rangle$ state form initially $|0\rangle + |+1\rangle$. (c) Total spin of the condensate initially prepared in $|+1\rangle$. (d) Decay curves for total number of condensed atoms in all m_F states, given for different initial m_F preparations.

parameter-dependent ground state spin composition of the system, reflecting its magnetic properties [28]. Theory predicts ^{87}Rb in $F=2$ to be in the polar phase, but close to the border to the so-called cyclic phase [19].

Experimentally we find the system dominated by three processes, setting different timescales, in increasing order: spin dynamics, two-body hyperfine losses and three-body recombination. This hierarchy allows us to separately analyze individual interaction processes, which are exemplarily given in Fig. 2.

In a first set of measurements we study the evolution of spinor condensates starting from different initial spin states. Figure 2(a) shows the evolution of the relative occupation of the different m_F components of a $F=2$ spinor condensate initially prepared in the state $|0\rangle$, also shown in Fig. 1(a). This example clearly demonstrates that spin evolution takes place predominantly between neighboring spin states, as expected from coupling via the dominating c_1 -term discussed above. Thus first the components $|\pm 1\rangle$ and only afterwards the $|\pm 2\rangle$ states are populated. Interestingly there is a delay in the occupation of $|\pm 1\rangle$ and a further delay in the occupation of $|\pm 2\rangle$ states. The latter delay can be intuitively explained since there must first be some occupation in the $|\pm 1\rangle$ states before the fully stretched states can be occupied. The origin of the initial delay as well as the "overshoot" of the $|\pm 1\rangle$ occupation is still under investigation.

As an interesting feature Fig. 2(a) shows evidence of spinor oscillations on a 100 ms timescale around equipartition. This indicates a coherent evolution between the

TABLE I: Spin evolution for different preparations.

initially prepared m_F states	initial total spin	initial channels into m_F state G [$10^{-13}\text{cm}^3\text{s}^{-1}$]	finally populated m_F states
$ 0\rangle$	0	$\rightarrow \pm 1\rangle \approx 21.0$	equipartition
$ +1\rangle + -1\rangle$	0	$\rightarrow 0\rangle \approx 26.9$ $\rightarrow \pm 2\rangle \approx 4.6$	equipartition
$ +1\rangle + 0\rangle + -1\rangle$	0	$\rightarrow \pm 2\rangle \approx 5.0$	equipartition
$ +2\rangle + -2\rangle$	0	-	$ +2\rangle + -2\rangle$
$ +2\rangle + 0\rangle + -2\rangle$	0	$\rightarrow \pm 1\rangle < 0.1$	$ +2\rangle + -2\rangle$
$ +2\rangle + -1\rangle$	1/2	-	$ +2\rangle$
$ +1\rangle + 0\rangle$	1/2	$\rightarrow +2\rangle \approx 21.7$ $\rightarrow -1\rangle \approx 19.2$ $\rightarrow +2\rangle \approx 22.4$ $\rightarrow 0\rangle \approx 12.2$ ($\rightarrow -1\rangle \approx 4.7$)	$ +2\rangle$
$ +1\rangle$	1	-	$ +2\rangle$
$ +2\rangle$	2	-	$ +2\rangle$

different m_F components, with only minor influence of the thermal cloud on this timescale.

In fact we always observe that spin dynamics is significantly quicker than thermalization. Spin dynamics thus leads to the formation of pure condensate wavefunctions in new spin states, which subsequently thermalize on a much longer timescale. This opens a new way to study thermalization effects with an independently tunable heat bath. In Fig. 2(b) the condensate and thermal fractions of the newly created $|+2\rangle$ state, starting with a mixture of the states $|+1\rangle$ and $|0\rangle$ are plotted. At first the condensate in the $|+2\rangle$ state is almost pure. This can be intuitively understood, as spin dynamics predominantly occurs in the high density condensate fraction on a timescale of the order of 25 ms. The subsequent buildup of a thermal cloud in the newly populated spin states takes place within a significantly longer time, of the order of 100 ms. Dominant effects contributing to the thermalization of the new spin state are the interaction of the new spin condensate with the parent thermal cloud ("melting"), and spin dynamics of the parent condensate fraction with the parent thermal cloud leading to a direct occupation of the new component thermal cloud. In this respect spinor condensates are a possible new tool for investigations of finite temperature effects.

In order to draw a more complete picture of spin dynamics in F=2 systems we now investigate the evolution of a variety of initial states as summarized in Table I. In this table we give estimates for the initial spin dynamics rates for different channels as well as the experimentally observed "final" distribution. The rates are intended for comparison with loss rates and between the different spin channel rates. They were obtained using the total ensemble density, number of BEC atoms in the prepared m_F components and the initial slope of a phenomenological exponential fit to the respective spin component population curves:

$$G_{\rightarrow|X\rangle} = \frac{dN_{|X\rangle}}{dt} \cdot \frac{N_{\text{initial}}}{\langle n_{\text{initial}} \rangle}.$$

At short timescales we find the rate for $|0\rangle \rightarrow |\pm 1\rangle$ similar to the rate $|\pm 1\rangle \rightarrow |0\rangle$ as one would expect for a reversible or coherent process. In contrast, at longer timescales the system evolves as expected into a time-independent distribution of m_F states. As a main result our measurements show the stability of a mixture of $|\pm 2\rangle$ (see Table I and Fig. 1(d)), for which we also find no spatial separation of the two components in the trapping volume. This is clear evidence of *polar behavior* as predicted for F=2 spinor condensates of ^{87}Rb .

Some initial preparations with zero total spin end up with all m_F components equally populated (see also Fig. 1(a,c)). This is in fact one of several degenerate ground states of the polar phase in the case of zero magnetic field [20], but the quadratic Zeeman energy lifts this degeneracy. For our experimental parameters a mixture of all m_F components is not a ground state for any phase in the mean-field description. The observed behavior might be due to a lack of time to reach the ground state, as spin-dependent losses depopulate the condensate before thermal equilibrium is reached.

Remarkably, if the atoms are prepared in superpositions which are ground states for the *cyclic phase* we observe very slow dynamics. First the mixture of $|+2\rangle + |0\rangle + |-2\rangle$, which is the ground state of the cyclic phase with total spin zero [20] shows nearly no spin dynamics. If starting with $|+2\rangle + |-1\rangle$ as a ground state for the cyclic phase at $B > 0$ [28] with non-zero spin we do not observe any spin dynamics. These cases are particularly surprising, as the states $|0\rangle$ alone as well as $|+1\rangle$ alone show fast spin dynamics as can be seen in Fig. 1(a,b). In the mixtures however, we observe only a faster decay of the $|0\rangle$ and $|-1\rangle$ component compared to $|\pm 2\rangle$. Concluding this, the stability of the $|\pm 2\rangle$ mixture demonstrates polar behavior of F=2 ^{87}Rb atoms, and in addition the slow dynamics of prepared cyclic ground states shows the F=2 state to be close to the cyclic phase [29].

An important point in the dynamics of spinor condensates is total spin conservation. This is directly observed in the rates for all spin preparations (see rates Table I) except in the case starting with $|+1\rangle$. Here we observe a much higher rate for the production of the $|+2\rangle$ atoms than for the ones in $|0\rangle$. This can be understood as follows: Imagine the $|0\rangle$ atoms favor to change their spin into $|-1\rangle$ while interacting with an atom in the initial spin state which then changes into $|+2\rangle$. Then the correct rates are determined by the measured values $G_{\rightarrow|+2\rangle} - G_{\rightarrow|-1\rangle}$ and $G_{\rightarrow|0\rangle} + G_{\rightarrow|-1\rangle}$. These two values are $17.7 \times 10^{-13}\text{cm}^3\text{s}^{-1}$ and $16.9 \times 10^{-13}\text{cm}^3\text{s}^{-1}$, respectively, and agree within the expected precision.

Investigating spinor condensates with initial spin $\neq 0$ one finds that the combination of spin dynamics and spin-dependent hyperfine losses (see below) leads to a loss induced magnetization during the evolution to the final

state (Fig. 1(b),2(c)). The remaining condensate always ends up in the fully stretched state if the initial state was prepared with non-zero total spin or in any other non-symmetric mixture. This is due to the fact that only the fully stretched component is immune to hyperfine-changing collisions. The magnetization process is only inhibited for a symmetric initial state having total spin zero.

Next we focus on hyperfine-changing collisions (i.e. involving transitions $F=2 \rightarrow F=1$) as a special case of spin relaxation dynamics. The release of hyperfine energy in these collisions leads to immediate loss of the collision partners from the trap. This loss process usually takes place on very short timescales, prohibiting the observation of spin dynamics in the upper hyperfine level, e.g. of ^{23}Na [15]. The relatively low hyperfine loss rates we find for ^{87}Rb are due to a coincidental destructive interference of decay paths [6, 30]. Fig. 2(d) shows the decay of Bose-Einstein condensates of ^{87}Rb prepared in different m_F states/mixtures. The decay of the stretched state $|+2\rangle$ is dominated by three-body recombination and was measured by [31] to be $L = 1.8 \times 10^{-29} \text{cm}^6 \text{s}^{-1}$, a value which also fits to our data. The equal superposition of the $|+2\rangle$ and $|-2\rangle$ states is special in the sense that we observe no spin dynamics in this case. The hyperfine-changing collisions can thus only occur via collisions of the type $|2, +2\rangle + |2, -2\rangle \rightarrow |1, m_1\rangle + |F, m_2\rangle (F = 1, 2)$. We deduce the two-body rate $G = 6.6(\pm 0.9) \times 10^{-14} \text{cm}^3 \text{s}^{-1}$, which leads to a much faster decay than three-body losses for the pure $|+2\rangle$ state (Fig. 2(d)). The dependence of the hyperfine-changing collision rate on the number of decay channels involved becomes obvious observing the decay of a condensate initially prepared in the state $|0\rangle$ (see Fig. 2(d)). It is important to note that in this case spin dynamics more rapidly ($\leq 25 \text{ms}$) distributes the population almost equally over all m_F states. The decay curve (of initially $|0\rangle$) thus effectively represents the loss of a spin state equipartition, which has access to all possible channels. We determine the mean two-body decay rate for this case to be $G = 10.2(\pm 1.3) \times 10^{-14} \text{cm}^3 \text{s}^{-1}$.

Finally we have also studied spinor condensates in the $F=1$ state where we observe slow spin dynamics on a timescale of seconds like in the case of ^{23}Na in $F=1$ [10]. Starting in the superposition state $|1, \pm 1\rangle$ we observe the creation of the $|1, 0\rangle$ component. The final state with all m_F components populated and spacially mixed is reached after about seven seconds. According to the phase diagrams of [10] we have thus shown that *^{87}Rb in the $F=1$ state is ferromagnetic* as predicted by [19].

In conclusion we have presented studies of various aspects of $F=2$ spinor condensates in ^{87}Rb . In particular we have discussed rates for spin dynamics as well as the evolution into the magnetic ground state. Furthermore we have investigated spin-dependent hyperfine-changing collisions and thermalization effects in newly created spin components during spinor evolution. These studies have

demonstrated the feasibility of ^{87}Rb condensates as a model for $F=2$ spin systems, added data to the collisional properties of ^{87}Rb and opened a new path for finite temperature studies. As a key result we measure ^{87}Rb in the $F=1$ state to be ferromagnetic and observe polar behavior for the $F=2$ state.

We acknowledge stimulating contributions by W. Ertmer and support from the *Deutsche Forschungsgemeinschaft* in the SFB 407 and the SPP 1116.

-
- [1] H. Pu and P. Meystre, Phys. Rev. Lett. **85**, pp. 3987 (2000).
 - [2] L. You and M. S. Chapman, Phys. Rev. A **62**, 052302 (2000).
 - [3] A. Sørensen, L.-M. Duan, J. I. Cirac, and P. Zoller, Nature **409**, pp. 63 (2001).
 - [4] B. Julsgaard, A. Kozhokin, and E. S. Polzik, Nature **413**, 400 (2001).
 - [5] O. Mandel et al., Phys. Rev. Lett. **91**, 010407 (2003).
 - [6] C. J. Myatt et al., Phys. Rev. Lett. **78**, 586 (1997).
 - [7] D. S. Hall et al., Phys. Rev. Lett. **81**, 1539 (1998).
 - [8] M. R. Matthews et al., Phys. Rev. Lett. **81**, 243 (1998).
 - [9] J. M. McGuirk et al., Phys. Rev. Lett. **89**, 090402 (2002).
 - [10] J. Stenger et al., Nature **396**, 345 (1999).
 - [11] H.-J. Miesner et al., Phys. Rev. Lett. **82**, 2228 (1999).
 - [12] D. M. Stamper-Kurn et al., Phys. Rev. Lett. **83**, 661 (1999).
 - [13] A. E. Leanhardt et al., Phys. Rev. Lett. **90**, 140403 (2003).
 - [14] M. D. Barrett, J. A. Sauer, and M. S. Chapman, Phys. Rev. Lett. **87**, 010404 (2001).
 - [15] A. Görlitz et al., Phys. Rev. Lett. **90**, 090401 (2003).
 - [16] C. V. Ciobanu, S.-K. Yip, and T.-L. Ho, Phys. Rev. A **61**, 033607 (2000).
 - [17] T.-L. Ho and L. Yin, Phys. Rev. Lett. **84**, 2302 (2000).
 - [18] M. Koashi and M. Ueda, Phys. Rev. Lett. **84**, 1066 (2000).
 - [19] N. N. Klausen, J. L. Bohn, and C. H. Greene, Phys. Rev. A **64**, 053602 (2001).
 - [20] M. Ueda and M. Koashi, Phys. Rev. A **65**, 063602 (2002).
 - [21] N. D. Mermin, Phys. Rev. A **9**, 868 (1974).
 - [22] E. G. van Kempen, S. J. Kokkelmans, D. J. Heinzen, and B. J. Verhaar, Phys. Rev. Lett. **88**, 093201 (2002).
 - [23] A. Marte et al., Phys. Rev. Lett. **89**, 283202 (2002).
 - [24] N. Poli, R. J. Brecha, G. Roati, and G. Modugno, Phys. Rev. A **65**, 021401R (2002).
 - [25] M.-O. Mewes et al., Phys. Rev. Lett. **78**, 582 (1997).
 - [26] Note that the desired initial state is preserved up to this time as spin dynamics at high magnetic field values is either energetically suppressed or releases enough quadratic Zeeman energy to eject the corresponding atoms from the trap.
 - [27] T.-L. Ho, Phys. Rev. Lett. **81**, 742 (1998).
 - [28] Detailed calculations on ground state properties including the quadratic Zeeman energy will be presented elsewhere.
 - [29] Note, there might be the option, that ^{87}Rb ($F=2$) is cyclic at $B=0$, but shifted into the polar phase by our small offset field of 340mG.

- [30] P. S. Julienne, F. H. Mies, E. Tiesinga, and C. J. Williams, Phys. Rev. Lett. **78**, 1880 (1997).
- [31] J. Söding et al., Appl. Phys. B **69**, 257 (1999).